Liquid Crystals
Publication details, including instructions for authors and subscription information:
http://www.tandfonline.com/loi/tlct20

Mesophase behaviour of binary mixtures of bell-shaped and calamitic compounds

D.Ž. Obadović [a], A. Vajda [b], A Jákli [c], A. Menyhárd [d], M. Kohout [e], J. Svoboda [e], M. Stojanović [a], N. Éber [b], G. Galli [f] & K. Fodor-Csorba [b]

[a] Department of Physics, Faculty of Sciences, University of Novi Sad, Trg D. Obradovića 4, Novi Sad, Serbia

[b] Research Institute for Solid State Physics and Optics, Hungarian Academy of Sciences, H-1525 Budapest, P.O. Box 49, Hungary

[c] Liquid Crystal Institute and Chemical Physics Interdisciplinary Program, Kent State University, Kent, OH, 44242, USA

[d] Department of Physical Chemistry and Material Science, Laboratory of Plastics and Rubber Technology, Budapest University of Technology and Economics, H-1521 Budapest, P.O. Box 91, Hungary

[e] Department of Organic Chemistry, Institute of Chemical Technology, Technicka 5, 166 28 Prague 6, Czech Republic

[f] Dipartimento di Chimica e Chimica Industriale, Università di Pisa, Via Risorgimento 35, Pisa, 56126, Italy

Version of record first published: 28 May 2010

To cite this article: D.Ž. Obadović, A. Vajda, A Jákli, A. Menyhárd, M. Kohout, J. Svoboda, M. Stojanović, N. Éber, G. Galli & K. Fodor-Csorba (2010): Mesophase behaviour of binary mixtures of bell-shaped and calamitic compounds, Liquid Crystals, 37:5, 527-536

To link to this article: http://dx.doi.org/10.1080/02678291003692672

Liquid Crystals,
Vol. 37, No. 5, May 2010, 527–536

Taylor & Francis
Taylor & Francis Group

Mesophase behaviour of binary mixtures of bell-shaped and calamitic compounds

D.Ž. Obadović[a], A. Vajda[b], A Jákli[c], A. Menyhárd[d], M. Kohout[e], J. Svoboda[e], M. Stojanović[a], N. Éber[b]*, G. Galli[f] and K. Fodor-Csorba[b]

[a]*Department of Physics, Faculty of Sciences, University of Novi Sad, Trg D. Obradovića 4, Novi Sad, Serbia;* [b]*Research Institute for Solid State Physics and Optics, Hungarian Academy of Sciences, H-1525 Budapest, P.O. Box 49, Hungary;* [c]*Liquid Crystal Institute and Chemical Physics Interdisciplinary Program, Kent State University, Kent, OH 44242, USA;* [d]*Department of Physical Chemistry and Material Science, Laboratory of Plastics and Rubber Technology, Budapest University of Technology and Economics, H-1521 Budapest, P.O. Box 91 Hungary;* [e]*Department of Organic Chemistry, Institute of Chemical Technology, Technicka 5, 166 28 Prague 6, Czech Republic;* [f]*Dipartimento di Chimica e Chimica Industriale, Università di Pisa, Via Risorgimento 35, Pisa 56126, Italy*

(*Received 8 December 2009; final version received 10 February 2010*)

A new bell-shaped compound, (dec-9-en-1-yl) 3,5-bis{[4'-(n-nonyloxy)biphenyl-4-carbonyl]oxy}benzoate (**I**), with symmetrical substitution in positions 3 and 5 of the central ring, was prepared. Although this material was not mesogenic, it exhibited low melting and freezing points and was therefore suitable as a component for mixing studies. These were carried out on a binary system composed of **I** and the rod-like 4-(n-octyloxy)phenyl 4-(n-hexyloxy)benzoate (**II**), which exhibits enantiotropic nematic, as well as monotropic SmC and SmX phases. Selected mixtures were studied by polarising optical microscopy, differential scanning calorimetry and X-ray diffraction on non-oriented samples. It was found that the binary mixtures exhibit mesomorphic properties close to room temperature.

Keywords: bent-core liquid crystal; binary mixtures; X-ray diffraction; electro-optics

1. Introduction

Bent-core (banana-shaped) compounds [1] represent a new class of thermotropic liquid crystals with a non-conventional architecture and an ability to exhibit mesomorphic properties (banana phases B_1–B_8) different from those of classical liquid crystals [2, 3]. Ferroelectric switching in an achiral liquid crystal was first observed in Schiff's base type banana compounds, which exhibited rich polymorphism [4]. This switchable polar phase was later found in more stable ester types of bent-core compounds [5, 6]. Inspired by their unusual properties, bent-core compounds have been investigated intensively in the last decade (see [7–10] and references cited therein).

In the search for materials with a new chemical architecture, modified bent-shaped compounds have also been synthesised which possess, in addition to the two lengthening arms, a third arm. Molecules with their arms connected in positions 1, 2 and 4 of the central benzene ring have been termed λ-shaped [11–13], while those with connections in positions 1, 3 and 5 have been called star like [14] or bell-shaped compounds [15]. Although these latter low melting-point substances usually did not exhibit mesogenic behaviour, they could be used as components for mixtures [14, 15].

Lowering the transition temperatures of bent-core liquid crystals has always been an important aim of studies, as these materials usually have high clearing points. Mixing compounds of different molecular structures has proven to be a useful tool to achieve lower transition temperatures in calamitic systems. Miscibility studies with bent-core compounds are, nevertheless, not yet as common as in calamitic liquid crystals. Some earlier studies have indicated only a limited miscibility of banana compounds. A way to escape this problem is to mix bent-core and calamitic molecules [14–20] which could lead to unusual self-assemblies [19, 20].

Here we report on the synthesis of a new bell-shaped compound, (dec-9-en-1-yl) 3,5-bis{[4′-(n-nonyloxy) biphenyl-4-carbonyl]oxy}benzoate (**I**), which is intended to be a starting material for the preparation of side-chain polymers. Inspired by former results [14] we carried out miscibility studies on the binary system of the bell-shaped compound **I** and the rod-like compound 4-(n-octyloxy)phenyl 4′-(n-hexyloxy)benzoate (**II**) [21]. The aim was to lower the clearing temperatures and to study the properties of such binary systems. We report on polarising optical microscopy (POM) and differential scanning calorimetry (DSC) studies as well as on X-ray measurements of the mixtures.

2. Synthesis

The synthesis of the bell-shaped compound (shown in Scheme 1) started with 3,5-dihydroxybenzoic acid (**1**).

*Corresponding author. Email: eber@szfki.hu

ISSN 0267-8292 print/ISSN 1366-5855 online

DOI: 10.1080/02678291003692672
http://www.informaworld.com

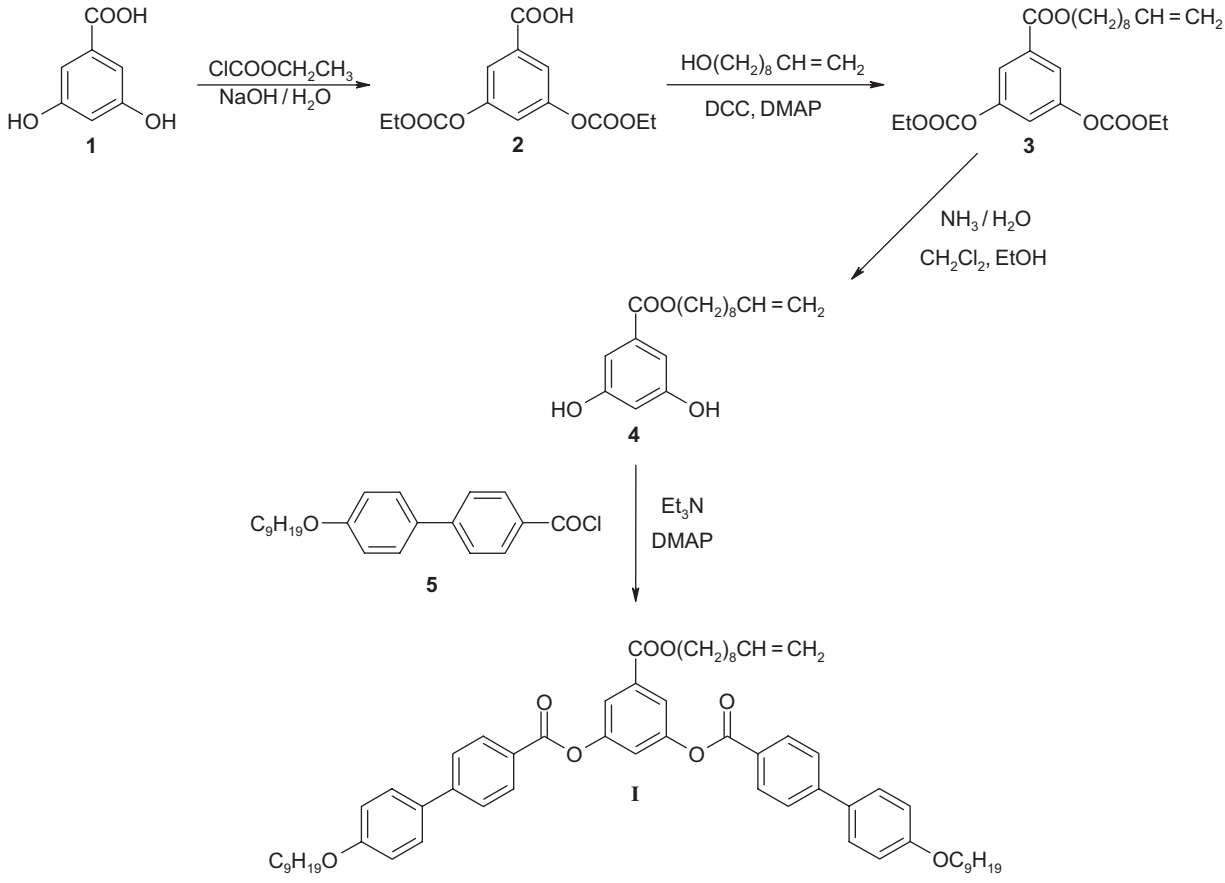

Scheme 1. Synthetic route for the (dec-9-en-1-yl) 3,5-bis{[4′-(n-nonyloxy)biphenyl-4-carbonyl]oxy}benzoate.

Acid **1** was first protected by ethoxycarbonyl groups using a known method [22]. The protected acid **2** was then esterified with dec-9-enol using a DCC mediated coupling. The following deprotection was achieved by diluted ammonia providing the central core compound **4** which was then lengthened with 4′-(n-nonyloxy)biphenyl-4-carbonyl chloride (**5**) to obtain the target material. The final product **I** was purified by flash chromatography (Kieselgel 60 0.063–0.02 mm) and multiple crystallisations from ethanol.

2.1 (Dec-9-en-1-yl) 3,5-bis{(ethoxycarbonyl)oxy} benzoate (3)

To a solution (0°C) of **2** (7.5 g; 25.2 mmol) in dry dichloromethane (100 ml), dec-9-enol (4.7 ml; 26.4 mmol) and a catalytic amount of DMAP (50 mg) were added followed by DCC (5.4 g; 26.4 mmol) in dry dichloromethane (15 ml). The reaction mixture was stirred at 0°C for 30 min and then decomposed with water (0.5 ml). The precipitate was filtered and the filtrate was evaporated. The crude product was purified by flash chromatography (hexane/ethyl acetate 6/1). 9.52 g (84%) of clear oil was obtained. ^{1}H NMR: 1.32 (m, 10 H), 1.39 (t, 6 H), 1.74 (m, 2 H), 2.04 (m, 2 H), 4.32 (m, 6 H), 4.95 (m, 2 H), 5.81 (m, 1 H), 7.32 (t, 1 H, $J = 2.4$), 7.75 (d, 2 H, $J = 2.4$). Elemental analysis: for $C_{23}H_{32}O_8$ (436.51), calculated C 63.29, H 7.39; found C 63.47, H 7.21%.

2.2 (Dec-9-en-1-yl) 3,5-dihydroxybenzoate (4)

To a solution of **3** (5.2 g; 11.9 mmol) in a mixture of dichloromethane (15 ml) and ethanol (90 ml), 25% aqueous ammonia solution (30 ml) was added. The reaction mixture was stirred at room temperature for 2.5 h, diluted with water (90 ml) and dichloromethane (30 ml), cooled to 0°C and acidified with 15% aqueous HCl to pH∼1. Layers were separated and the water layer was extracted with dichloromethane (2 × 30 ml). The combined organic solution was washed with water (2 × 30 ml), saturated solution of NaCl (30 ml) and dried with anhydrous magnesium sulphate. The solvent was evaporated and the crude oily product was

purified by flash chromatography (hexane/ethyl acetate 2/1). Yield 2.90 g (82%) of **4**. ^{1}H NMR: 1.35 (m, 10 H), 1.72 (m, 2 H), 2.03 (m, 2 H), 4.27 (t, 2 H), 4.75 (bs, 2 H), 4.95 (m, 2 H), 5.80 (m, 1 H), 6.60 (t, 1 H, $J = 2.1$), 7.09 (d, 2 H, $J = 2.1$). Elemental analysis: for $C_{17}H_{24}O_4$ (292.38), calculated C 69.84, H 8.27; found C 69.56, H 7.98%.

2.3 (Dec-9-en-1-yl) 3,5-bis{[4′-(n-nonyloxy)biphenyl-4-carbonyl]oxy}benzoate (I)

To a solution of hydroxy ester **4** (0.35 g; 1.14 mmol), Et_3N (0.4 ml; 2.90 mmol) and a catalytic amount of DMAP (50 mg) in dry dichloromethane (35 ml), a solution of acid chloride **5** in dry dichloromethane (15 ml) was added. The reaction mixture was stirred at room temperature for 30 min and decomposed with water (50 ml). Layers were separated and the water layer was washed with dichloromethane (2 × 30 ml). The combined organic solution was washed with 5% aqueous HCl (20 ml), water (30 ml), saturated solution of NaCl and dried with anhydrous magnesium sulphate. The solvent was evaporated and the crude product was purified by flash chromatography (toluene). Yield: 0.87 g (81%) of **I** was obtained. ^{1}H NMR: 0.88 (t, 6 H), 1.23–1.53 (m, 34 H), 1.77 (m, 2 H), 1.82 (m, 4 H), 2.03 (m, 2 H), 4.02 (t, 4 H), 4.34 (t, 2 H), 4.95 (m, 2 H), 5.80 (m, 1 H), 7.00 (d, 4 H, $J = 8.8$), 7.45 (t, 1 H, $J = 2.2$), 7.60 (d, 4 H, $J = 8.8$), 7.70 (d, 4 H, $J = 8.6$), 7.85 (t, 2 H, $J = 2.2$), 8.23 (d, 4 H, $J = 8.6$). Elemental analysis: for $C_{61}H_{76}O_8$ (937.28), calculated C 78.17, H 8.17; found C 78.03, H 8.21%.

3. Mixtures of bell-shaped and rod-like compounds

The goal of the present study was to test the miscibility of the bell-shaped compound **I** with the rod-like material **II**, and to study the mesomorphic behaviour of their binary mixtures. The chemical structures and phase sequences of the studied materials are depicted in Figure 1.

For the detailed study, five mixtures, **Mix1** to **Mix5,** have been prepared with 8.5, 20, 41, 50 and 67 wt% of the bell-shaped component, respectively.

3.1 Mesomorphic properties

The mesomorphic properties of the pure compounds and their mixtures were investigated by POM using an Amplival Pol-U microscope equipped with a Boetius hot stage. The heating rate was 4°C/min; the cooling rate was not controlled (free cooling). Phase transition temperatures were also checked by DSC (Pyris Diamond Perkin-Elmer 7) using samples of 3–8 mg hermetically sealed in aluminium pans and nitrogen as purging gas (20 ml/min). The equipment was calibrated with indium and zinc reference materials. The results indicated that the melting characteristics of the materials depend on the preparation conditions and the thermal history. In order to eliminate the effect of this history the samples were heated from 0°C up to 100°C with a heating rate of 20°C/min. The structural changes and the crystallisation characteristics of the samples were then studied during slow cooling from 100°C to 0°C with a cooling rate of 1°C/min. The melting characteristics after slow cooling were finally studied during reheating of the samples again to 100°C with a heating rate of 4°C/min. The phase transition temperatures obtained by POM and DSC with similar heating and cooling rates are in a good agreement.

The phase transition temperatures and enthalpies of the pure compounds and their mixtures are presented in Tables 1 and 2 for heating and for cooling, respectively**.** For a better illustration of the polymorphism the binary phase diagram of the system is also provided in Figures 2(a) and (b). The bell-shaped

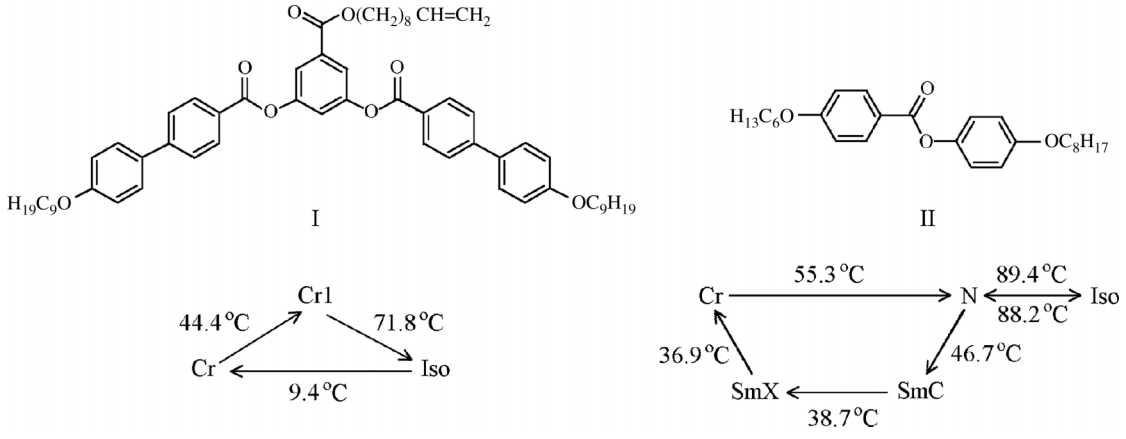

Figure 1. Structural formulae and phase transition temperatures of compounds **I** and **II**.

Table 1. Phase transition temperatures (T in °C) and transition enthalpies (ΔH in J/g) evaluated on heating with differential scanning calorimetry (DSC) and/or with polarising optical microscopy.

Code	Cr	T(°C) [ΔH(J/g)]	Cr_1	T(°C) [ΔH(J/g)]	N	T (°C) [ΔH(J/g)]	Iso
II	•	55.3 [86.9]	—		•	89.4 [5.3]	•
Mix1 (8.5 wt% of **I**)	•	46.3 [9.3]	•	53.1 [76.6]	•	84.9 [5.4]	•
Mix2 (20 wt% of **I**)	•	41.4 [11.6]	•	52.3 [71.4]	•	80.8 [4.0]	•
Mix3 (41 wt% of **I**)	•	41.8 [31.5]	•	48.9 [48.4]	•	70[a] [-]	•
Mix4 (50 wt% of **I**)	•	40.9 [43.3]	•	46.5 [17.1]	•	61[a] [-]	•
Mix5 (67 wt% of **I**)	•	40.5 [30.7]	•	45 [25.6]	•	60.8 [25.5]	•
I	•	44.4 [7.5]	•	71.8 [43.0]	—		•

Note: [a]Microscopy observation only (no DSC peak); enthalpy data are not available.

Table 2. Phase transition temperatures (T in °C) and transition enthalpies (ΔH in J/g) evaluated on cooling with differential scanning calorimetry (DSC) and/or polarising optical microscopy.

Code	Iso	T (°C) [ΔH(J/g)]	N	T (°C) [ΔH (J/g)]	SmC	T (°C) [ΔH (J/g)]	SmX	T (°C) [ΔH (J/g)]	Cr
II	•	88.2 [–5.6]	•	46.7 [–2.0]	•	38.7 [-][b]	•	36.9 [–83.2]	•
Mix1 (8.5 wt% of **I**)	•	84.0 [–3.4]	•	36.6 [–80.5][c]	•	35.4	•	34.0	•
Mix2 (20 wt% of **I**)	•	80.4 [–4.8]	•	34.7 [–34.8]	•	22.3 [-][b]	•	17.5 [–29.5]	•
Mix3 (41 wt% of **I**)	•	69[a] [-]	•	27.1 [–19.1]	•		—	16.9 [–55.36]	•
Mix4 (50 wt% of **I**)	•	60[a] [-]	•		—		—	10.4 [-][b]	•
Mix5 (67 wt% of **I**)	•	34.0 [-][b]	•		—		—	6.2 [–32.5]	•
I	•	9.4 [–22.3]	—		—		—	—	•

Note: [a]Microscopy observation only (no DSC peak); enthalpy data are not available.
[b]The intensity of the DSC peak is comparable with the sensitivity; reliable enthalpy data are not available.
[c]The close transitions are overlapping; only the overall enthalpy could be given.

compound **I** was not mesogenic; its isotropic (Iso) phase could, however, be undercooled considerably (by 60°C) below its melting point. This feature might be related to the molecular shape and size of compound **I**. A similar behaviour is quite common among polymers. The calamitic component **II** showed an enantiotropic nematic (N), as well as a monotropic smectic C (SmC) phase. In addition, a previously not reported lower temperature smectic X (SmX) phase was also observed by POM and DSC, as well as by X-ray diffraction (see Figure 3(a)). All prepared mixtures formed an enantiotropic nematic phase**.** The Iso→N phase transition temperatures decrease with increasing content of the bell-shaped compound **I**. The remarkable undercoolability of the Iso→N phase transition below the clearing point observed in **Mix5** might be inherited from compound **I** which constitutes a large part of the mixture. The SmX phase appears only in **Mix1** and **Mix2**, SmC is detectable in **Mix3** as well. Both smectic phases are monotropic in the mixtures, just as in the pure calamitic **II**.

3.2 X-ray diffraction

In order to help phase identification, non-oriented samples were investigated by X-ray diffraction in a transmission geometry using a conventional powder diffractometer, Seifert V-14, with CuKα radiation at $\lambda = 0.154$ nm, equipped with an automatic high-temperature kit Paar HTK-10.

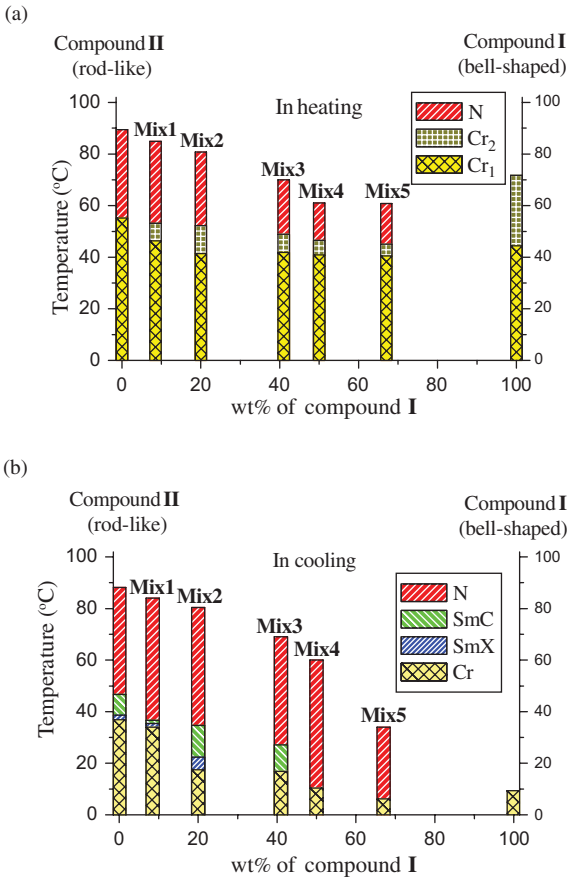

Figure 2. Phase diagram of the binary system composed of compounds **I** and **II** obtained by differential scanning calorimetry (DSC) and/or polarising optical microscopy (POM): (a) in heating; and (b) in cooling.

Diffraction studies were carried out on the calamitic compound **II**, as well as on the binary mixtures. Two parameters characteristic for molecular packing, the thickness of the smectic layers d (if layers exist) and the average intermolecular distance D between the long axes of neighbouring molecules [10, 16, 17, 23], could be determined from the positions of the small-angle and wide-angle diffraction peaks, respectively. The evaluation was based on the Bragg law: $n\lambda = 2d \sin \theta$, where λ is the radiation wavelength, θ is the scattering angle and d is the repetition distance to be determined. These results are summarised in Table 3. In Figures 3(a) and 3(b) we present typical diffraction spectra for each phase of the pure calamitic compound **II** as well as for the mixture **Mix3**, in order to demonstrate the change occurring in the phase transitions. Both the isotropic and the nematic phases are characterised by a broad diffusion peak which appears in the range of $2\theta = 12$–$26°$. In the SmC phase of **II**, one reflection peak appears at the small angle $2\theta = 3.4°$, related to the smectic layers. On further decreasing the temperature another reflection becomes detectable at $2\theta \sim 19.7°$, superimposed on the broad diffusion peak. This indicates the appearance of an order in the smectic layer plane, i.e. a transition to another, although not yet identified, SmX phase. Although the smectic layer thickness in the SmX phase is slightly larger compared with that in the SmC phase (as seen in Table 3), it is still much smaller than the length of the molecule shown in Figure 4. This implies that SmX is a kind of tilted smectic phase with a tilt angle of about 30°. At even lower temperatures, below crystallisation, the diffraction profile becomes much more complex with many reflection peaks. Analysis of the diffraction profiles has shown that the centre of the broad diffraction peak shifts slightly toward larger angles with reducing the temperature. This indicates that average intermolecular distance D decreases during the successive phase transitions on cooling, i.e. the packing becomes slightly denser.

In the studied mixtures SmC phase, characterised by one reflection at a small angle, could be detected in **Mix1–Mix3** only. The positions of the peak were slightly shifted compared with that of the rod-like molecule. The analysis of the X-ray diffraction profile showed a decrease in the smectic layer thickness d with the increase in the concentration of bell-shaped molecules in the mixture (see Table 3).

The lower temperature SmX could be observed only in **Mix1** and **Mix2**. The intense peak which was superimposed on the broad diffusion peak at $2\theta \sim 19.0°$ and 18.9°, respectively, indicates the appearance of intralayer ordering, similarly to that in compound **II**.

The increase in the concentration of bell-shaped molecules causes, in the isotropic phase, a slight shift of the centre of the broad diffuse peak towards larger 2θ values, i.e. an increase of the molecule packing density (a decrease in D). A similar effect has not been observed, however, in the N and SmC phases; there, D retains its constant value in all studied mixtures where these phases existed.

3.3 Molecular calculations

Molecular models were constructed in order to give us an insight into the problematic self-assembly of the bell-shaped and calamitic materials in the mesophase. Computation was performed with Gaussian 03 software [24] using a density functional theory (DFT) method with the B3LYP 6–31G base set. The results of computation were then compared with the X-ray measurements.

The calamitic compound (Figure 4) was found to be almost planar, the twist between phenyl rings is only 9°. On the other hand, the molecule is not completely linear but has a slightly bent structure which

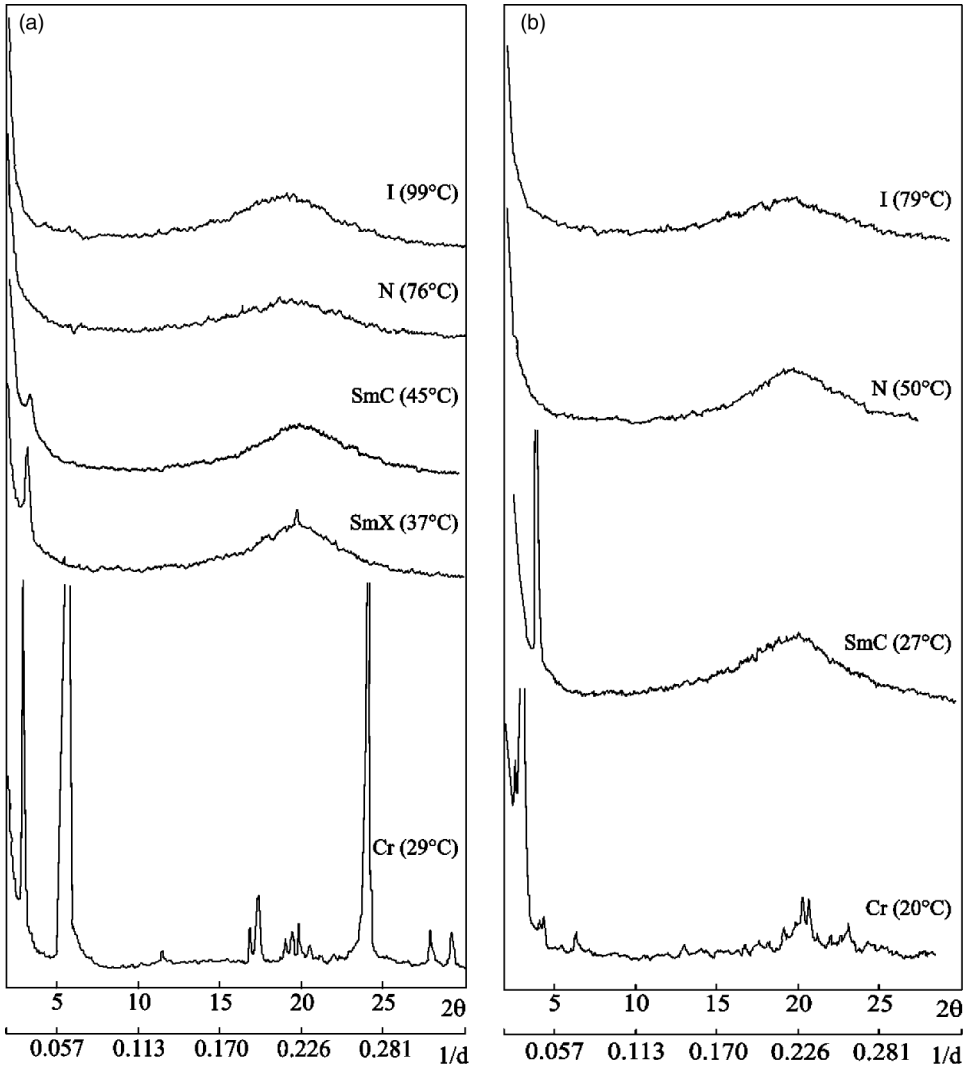

Figure 3. X-ray diffraction profiles for: (a) the rod-like molecule **II**; (b) the mixture **Mix3**.

might be helpful for the self-assembly with the bell-shaped compound in the mesophase.

The three phenyl rings in the centre of the bell-shaped molecule (Figure 5) are in a plane. Also the alkenyl chain on the top of the molecule is located almost in the same plane, only the double bond is pointing out to the space. The outer biphenyl rings are twisted by 35°. The terminal alkyl chains are in the plane of these outer aryl units. The bend angle between the biphenyl units is only 79° and the angle between the terminal carbons of the side chains is even smaller, 76°. This is caused by the deviation of the side chains from the axis of the biphenyl units.

Furthermore, we tried to establish a model of a possible assembly of these two molecular motifs in a smectic phase (Figure 6). The layer thickness of the SmC phase of **Mix3** is 2.26 nm, thus the tilt angle is approximately 57° for the bell-shaped compound **I** and it is 43° for the calamitic **II**. We assume that the calamitic molecules of **II** are held together by π–π stacking, while the terminal alkyl chains are most probably responsible for the interaction with the bell-shaped compound **I**. Other arrangements, where the calamitic compounds are not in a line, seem to be less advantageous. For a more precise insight into the SmC phase of **Mix3** one should set up a molecular dynamic model.

3.4 Electro-optical and polarisation current measurements

Electro-optical and polarisation current measurements were performed on planar aligned sandwich cells of **Mix2** and **Mix3**. Either homemade 5-μm-thick cells or 8-μm-thick commercially available cells (E.H.C. Co., Japan) were used. For both types the

Table 3. Molecular parameters of the investigated mixtures for all observed phases at a fixed temperature T (°C): angles corresponding to the reflection peaks 2θ (degrees), effective layer thickness d (in nm; error of measurements was $\delta_d \approx \pm 0.01$ nm), average repeat distance D (in nm; error of measurements was $\delta_D \approx \pm 0.02$ nm).

Mixture	Molar ratio I:II	T (°C)	2θ (°)	d (nm)	D (nm)
II	-	99 (Iso)	18.9		0.47
		76 (N)	19.1		0.46
		45 (SmC)	3.4	2.60	
			19.8		0.45
		37 (SmX)	3.3	2.67	
			19.7		0.45
Mix1 (8.5 wt% of **I**)	~1:25	102 (Iso)	18.9		0.47
		76 (N)	19.2		0.46
		36 (SmC)	3.45	2.56	
			19.7		0.45
		35 (SmX)	3.4	2.60	
			19.0		0.47
Mix2 (20 wt% of **I**)	~1:9	106 (Iso)	19.1		0.46
		76 (N)	19.3		0.46
		34 (SmC)	3.8	2.32	
			19.7		0.45
		22 (SmX)	3.7	2.39	
			18.9		0.47
Mix3 (41 wt% of **I**)	~1:3	79 (Iso)	19.5		0.45
		50 (N)	19.4		0.46
		27 (SmC)	3.9	2.26	
			19.5		0.45
Mix4 (50 wt% of **I**)	~1:2	68 (Iso)	19.6		0.45
		35 (N)	19.7		0.45
Mix5 (67 wt% of **I**)	~1:1	53 (Iso)	19.8		0.45
		33 (N)	19.9		0.45

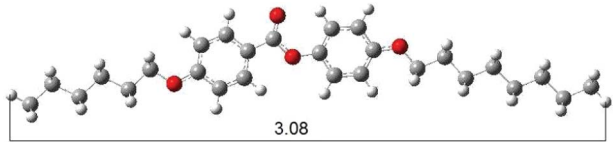

Figure 4. The model of compound **II** with the calculated length (in nm) of the molecule.

planar alignment was provided by antiparallel rubbed polyimide coatings. The liquid crystal cells were placed into a computer-controlled hot stage (STC200F from INSTEC) and the phase sequences were investigated by a polarising microscope (BX60 from Olympus). The set up for electric current measurements and electro-optical studies consisted of a digital oscilloscope (HP 54600B), a digital multimeter (HP 34401A) and an arbitrary waveform generator (HP 33120A).

As an example of electric current measurements, in Figure 7 we show the temporal variation $I(t)$ of the electric current flowing through the sample due to an applied voltage $V(t)$ of triangular waveform for the mixture **Mix2** (20 wt% of **I**). As seen, the current is composed of two contributions ($I = I_C + I_\Omega$). The capacitive current

$$I_C = \varepsilon_o \varepsilon \frac{A}{L} \cdot \frac{dV}{dt},$$

is responsible for the jumps seen in $I(t)$ at the peaks of the voltage waveform, since I_C changes sign as the slope of $V(t)$ is reversed. Here ε_0 is the permittivity of the vacuum, ε is the effective dielectric constant of the material, A is the electrode area and L is the sample thickness. In the periods of linearly increasing (decreasing) voltage the current is proportional to the voltage, simply corresponding to Ohm's law: $I_\Omega = V\sigma A/L$ (here σ is the conductivity of the liquid crystalline material). This shows the absence of ferroelectric polarisation (a purely dielectric response).

Representative POM textures of the same 8-μm-thick cell are presented in Figure 8. Figures 8(a)–(c)

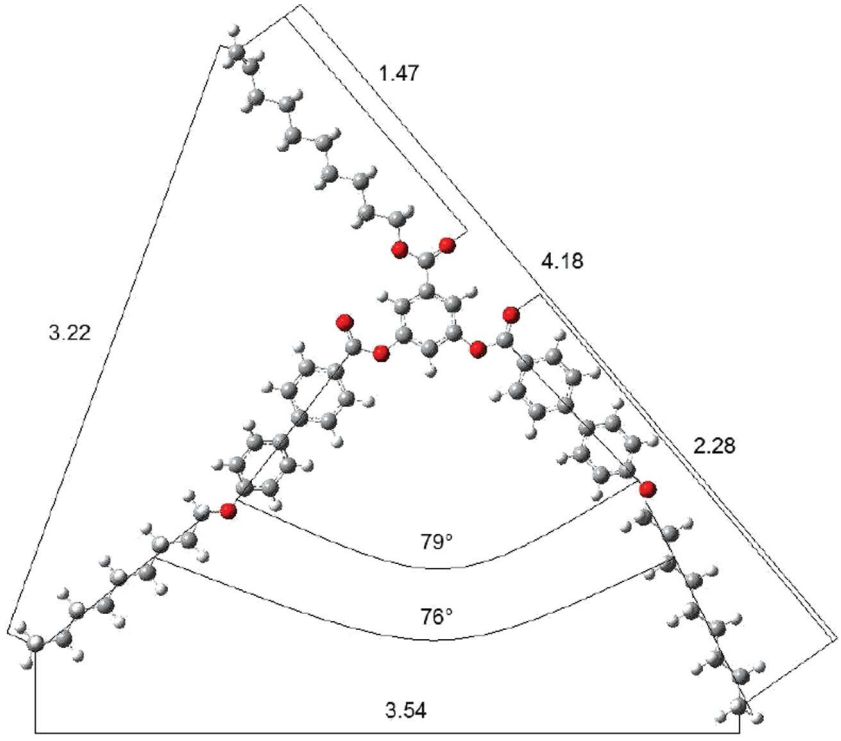

Figure 5. The model of compound **I** with the calculated bending angles and lengths (in nm) of different arms.

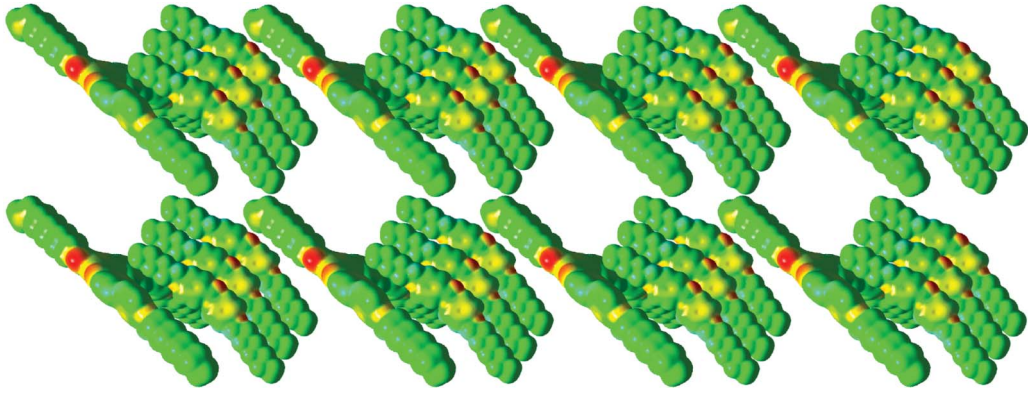

Figure 6. A model of a possible self-assembly of the bell-shaped and calamitic compounds in the SmC phase of **Mix3**. The electron density of the individual parts of the molecule is highlighted in colours (red, the highest; blue, the lowest) (colour version online).

show the uniformly aligned nematic phase at decreasing temperatures: at 75, 70 and 61°C, respectively. The colour changes are due to the temperature dependence of the refractive indices. Figure 8(d) shows the crystalline dendrites as they grew from one nucleation centre in the middle of the picture at 35°C. We note that the nematic phase could be supercooled into a metastable state even at the latter temperature, and crystallisation was initiated by pressing the cell. The monotropic (and also metastable) SmC and SmX phases did not appear in these measurements.

In the case of **Mix3** (41 wt% of bell-shaped molecules **I**), the temperature dependences of the optical transmittance of a cell between crossed polarisers are presented in Figure 9. We see that there is a 2°C-wide two-phase region at the isotropic–nematic (Iso–N) transition with a strong light scattering.

Typical textures of **Mix3** at different temperatures are presented in Figure 10. Figure 10(a) shows the defects generated at the Iso–N phase transition, Figures 10(b) and (c) are typical uniform textures in the nematic phase at 50.6 and 40°C, respectively. The sample remains in the nematic phase down to ~27°C, where it goes to a SmC phase, which is stable below room temperature. The focal conic texture of this SmC phase is shown in Figure 10(d) at 26°C.

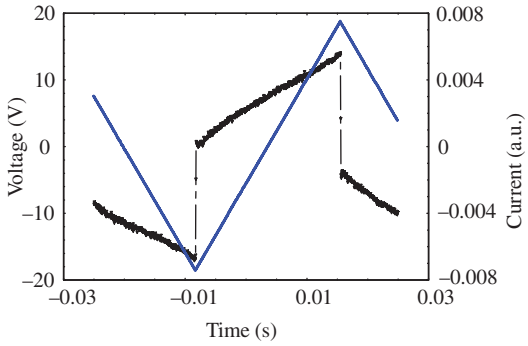

Figure 7. Time dependence of the electric current flowing through an 8-μm cell due to a triangular electric voltage at 75°C in **Mix2.**

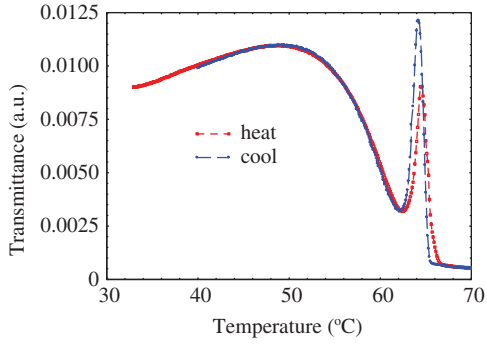

Figure 9. Temperature dependence of the optical transmittance at 2°C/min heating/cooling rates in **Mix3**.

In the nematic phase (i.e. above 27°C) the sample showed electro-hydrodynamic instabilities at low frequencies. A representative electroconvection pattern is presented in Figure 11. It depicts oblique roll morphology [25], often seen in nematics with negative

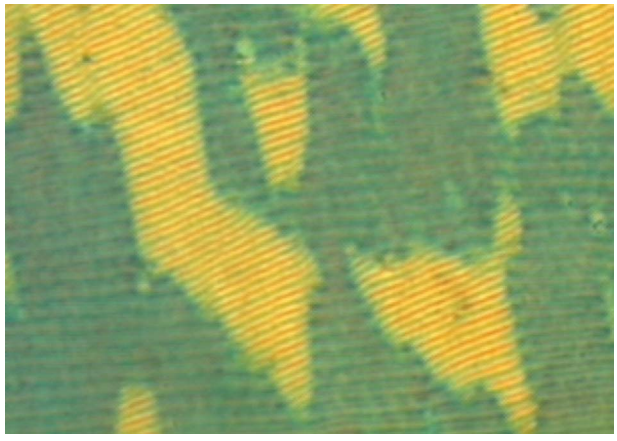

Figure 11. Electro-hydrodynamic instability in a **Mix3** sample under 15-V, 1-Hz, triangular voltage at 55°C.

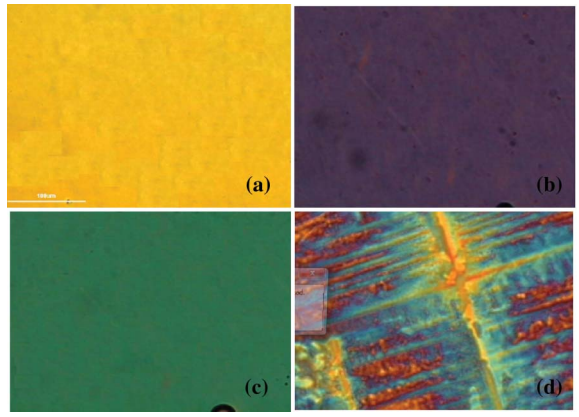

Figure 8. Representative textures of an 8-μm-thick planar cell of **Mix2**. The nematic phase at: (a) 75°C; (b) 70°C; (c) 61°C; and (d) crystalline texture formed after pressing the cell at 35°C.

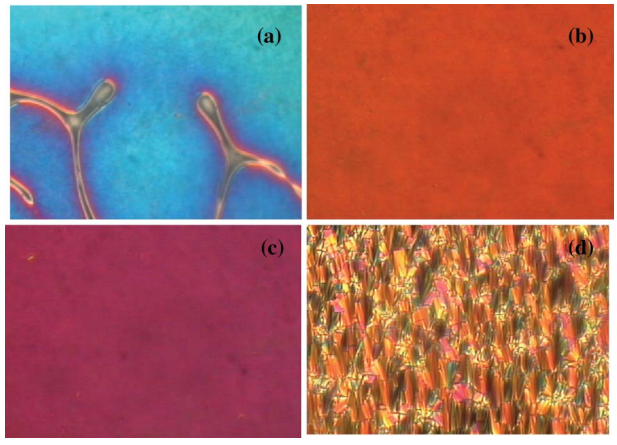

Figure 10. Representative textures of **Mix3** at different temperatures: in the N phase at: (a) 63°C; (b) 50.6°C; (c) 40°C; and (d) in the SmC phase at 26°C. Pictures cover an area of 0.4 mm × 0.3 mm.

dielectric and positive conductivity anisotropies ($\Delta\varepsilon < 0$, $\Delta\sigma > 0$).

Electric current measurements on **Mix3** show a purely dielectric type response both in the nematic and the SmC phases, similar to the case of **Mix2**.

4. Conclusions

The present studies were performed with the aim of contributing to the understanding of how mixing of bell-shaped and rod-like molecules affect the mesomorphic properties. Based on POM, DSC, X-ray and electro-optical measurements on several mixtures, we have found that the polymorphism (Iso–N–SmC–SmX phase sequence) of the pure calamitic component **II** is

fully preserved in the mixtures with high calamitic content (**Mix1**, **Mix2**). The layer spacing (*d*) decreases when adding the bell-shaped compound. On increasing the fraction of bell-shaped molecules the monotropic smectic phases gradually disappear (SmX by 41 wt%, SmC by 50 wt% of **I**). The enantiotropic nematic phase remains detectable even for the highest bell-shaped content (67 wt% of **I**). Therefore, mesophase behaviour existed over a broad compositional range in the mixtures and could be extended close to room temperature. The results suggest that combining conventional calamitics with bell-shaped mesogens with an appropriate molecular design may be a tool to tune the phase behaviour and properties of different liquid crystal mixtures.

Acknowledgements

This work has been supported by Grant No. 141020 from the Ministry of Science and Environmental Protection of the Republic of Serbia, the Hungarian Research Funds OTKA K61075, the ESF-COST D35 WG-13/05, COST D35 WG13/05 STSM 03524, the SASA-HAS bilateral scientific exchange project #2, Czech-Hungarian bilateral exchange, Grants No. 202/03/P011, No. 202/09/0047 from the Grant Agency of the Czech Republic and No. OC176 from the Ministry of Education, Youth and Sports of the Czech Republic.

References

[1] Niori, T.; Sekine, T.; Watanabe, J.; Furukawa, J.; Takezoe, H. *J. Mater. Chem.* **1996**, *6*, 1231–1233.
[2] Amaranatha Reddy, R.; Tschierske, C. *J. Mater. Chem.* **2006**, *16*, 907–961.
[3] Takezoe, H.; Takanishi, Y. *Jpn. J. Appl. Phys.* **2006**, *45*, 597–625.
[4] Pelzl, G.; Diele, S.; Weissflog, W. *Adv. Mater.* **1999**, *11*, 707–724.
[5] Fodor-Csorba, K.; Vajda, A.; Galli, G.; Jákli, A.; Demus, D. *Macromol. Chem. Phys*. **2002**, *203*, 1556–1563.
[6] Kohout, M.; Svoboda, J.; Novotná, V.; Glogarová, M.; Pociecha, D.; Gorecka, E. *J. Mater. Chem.* **2009**, *19*, 3153–3160.
[7] Jákli, A.; Krüerke, D.; Sawade, H.; Heppke, G. *Phys. Rev. Lett.* **2001**, *86*, 5715–5718.
[8] Dunemann, U.; Schröder, M.W.; Amarantha Reddy, R.; Pelzl, G.; Diele, S.; Weissflog, W. *J. Mater. Chem.* **2005**, *15*, 4051–4061.
[9] Goc, F.; Selbmann, Ch.; Rauch, S.; Heppke, G.; Dabrowski, R. *Mol. Cryst. Liq. Cryst*. **2005**, *439*, 147–160.
[10] Weissflog, W.; Shreenivasa Murthy, H.N.; Diele, S.; Pelzl, G. *Phil. Trans. R. Soc. A* **2006**, *364*, 2657–2679.
[11] Braun, D.; Reubold, M.; Schneider, L.; Wegmann, M.; Wendorff, J.H. *Liq. Cryst*. **1994**, *16*, 429–443.
[12] Yamaguchi, A.; Nishiyama, I.; Yamamoto, J.; Yokoyama, H.; Yoshizawa, A. *J. Mater. Chem.* **2005**, *15*, 280–288.
[13] Yamaguchi, A.; Yoshizawa, A.; Nishiyama, I.; Yamamoto, J.; Yokoyama, H. *Mol. Cryst. Liq. Cryst.* **2005**, *439*, 85–95.
[14] Bubnov, A.; Hamplová, V.; Kašpar, M.; Vajda, A.; Stojanovic, M.; Obadovic, D.Ž.; Éber, N.; Fodor-Csorba, K. *J. Thermal Anal. Calorimetry* **2007**, *90*, 431–441.
[15] Obadović, D.Z.; Vajda, A.; Jákli, A.: Kohout, M.; Stojanović, M.; Éber, N.; Fodor-Csorba, K.; Galli, G. *J. Res. Phys.* **2008**, *32*, 69–74.
[16] Schröder, M.W.; Diele, S.; Pelzl, G.; Pancenko, N.; Weissflog, W. *Liq. Cryst*. **2002**, *29*, 1039–1046.
[17] Takanishi, Y.; Shin, G.J.; Jung, J.C.; Choi, S.W.; Ishikawa, K.; Watanabe, J.; Takezoe, H.; Toledano, P. *J. Mater. Chem.* **2005**, *15*, 4020–4024.
[18] Nair, G.; Bailey, Ch.A.; Taushanoff, S.; Fodor-Csorba, K.; Vajda, A.; Varga, Z.; Bóta, A.; Jákli, A. *Adv. Mater.* **2008**, *20*, 3138–3142.
[19] Pratibha, R.; Madhusudana, N.V.; Sadashiva, B.K. *Science* **2000**, *288*, 2184–2187.
[20] Pratibha, R.; Madhusudana, N.V.; Sadashiva, B.K. *Phys. Rev. E* **2005**, *71*, 011701/1–12.
[21] van Meter, J.P.; Klanderman, B.H. *Mol. Cryst. Liq. Cryst.* **1973**, *22*, 271–284.
[22] Larrouquere J. *Bull. Soc. Chim. Fr.* **1968**, *1*, 329–335.
[23] Obadović, D.Ž.; Bata, L.; Tóth-Katona, T.; Bóta, A.; Fodor-Csorba, K.; Vajda, A.; Stančić, M. *Mol. Cryst. Liq. Cryst*. **1997**, *303*, 85–96.
[24] Frisch, M.J.; Trucks, G.W.; Schlegel, H.B.; Scuseria, G.E.; Robb, M.A.; Cheeseman, J.R.; Montgomery, J.A.; Vreven, T.; Kudin, K.N.; Burant, J.C.; Millam, J.M.; Iyengar, S.S.; Tomasi, J.; Barone, V.; Mennucci, B.; Cossi, M.; Scalmani, G.; Rega, N.; Petersson, G.A.; Nakatsuji, H.; Hada, M.; Ehara, M.; Toyota, K.; Fukuda, R.; Hasegawa, J.; Ishida, M.; Nakajima, T.; Honda, Y.; Kitao, O.; Nakai, H.; Klene, M.; Li, X.; Knox, J.E.; Hratchian, H.P.; Cross, J.B.; Bakken, V.; Adamo, C.; Jaramillo, J.; Gomperts, R.; Stratmann, R.E.; Yazyev, O.; Austin, A.J.; Cammi, R.; Pomelli, C.; Ochterski, J.W.; Ayala, P.Y.; Morokuma, K.; Voth, G.A.; Salvador, P.; Dannenberg, J.J.; Zakrzewski, V.G.; Dapprich, S.; Daniels, A.D.; Strain, M.C.; Farkas, O.; Malick, D.K.; Rabuck, A.D.; Raghavachari, K.; Foresman, J.B.; Ortiz, J.V.; Cui, Q.; Baboul, A.G.; Clifford, S.; Cioslowski, J.; Stefanov, B.B.; Liu, G.; Liashenko, A.; Piskorz, P.; Komaromi, I.; Martin, R.L.; Fox, D.J.; Keith, T.; Al-Laham, M.A.; Peng, C.Y.; Nanayakkara, A.; Challacombe, M.; Gill, P.M.W.; Johnson, B.; Chen, W.; Wong, M.W.; Gonzalez, C.; Pople, J.A. Gaussian, Inc., Wallingford, CT, 2004.
[25] Kramer, L.; Pesch, W. In *Pattern Formation in Liquid Crystals*: Buka, A., Kramer, L., Eds.; Springer: New York, 1996; pp 221–255.